

Supporting information

Silver Nanoparticles with exceptional near-infrared absorbance for photo-enhanced antimicrobial applications

Connor R. Bourgonje, Daliane R.C. Silva, Ella McIlroy, Nicholas D. Calvert, Adam J. Shuhendler, Juan C. Scaiano

Department of Chemistry and Biomolecular Sciences, University of Ottawa, Ottawa, Ontario, Canada K1N 6N5

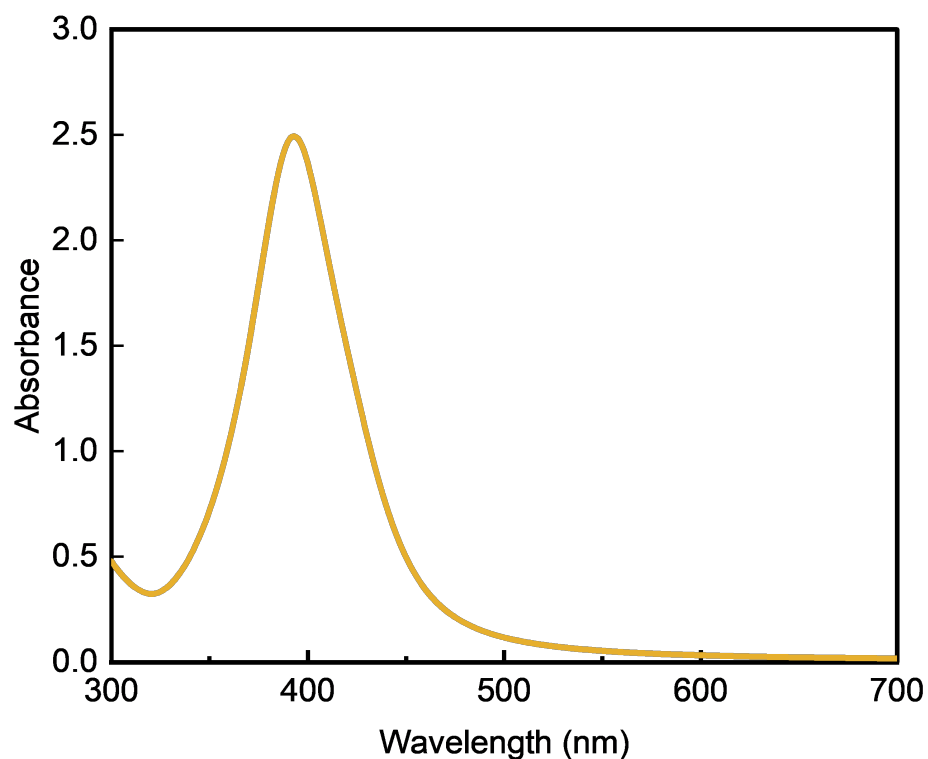


Figure S1: UV-Vis absorption spectrum of aqueous AgNP seeds following UV photoreduction of AgNO₃.

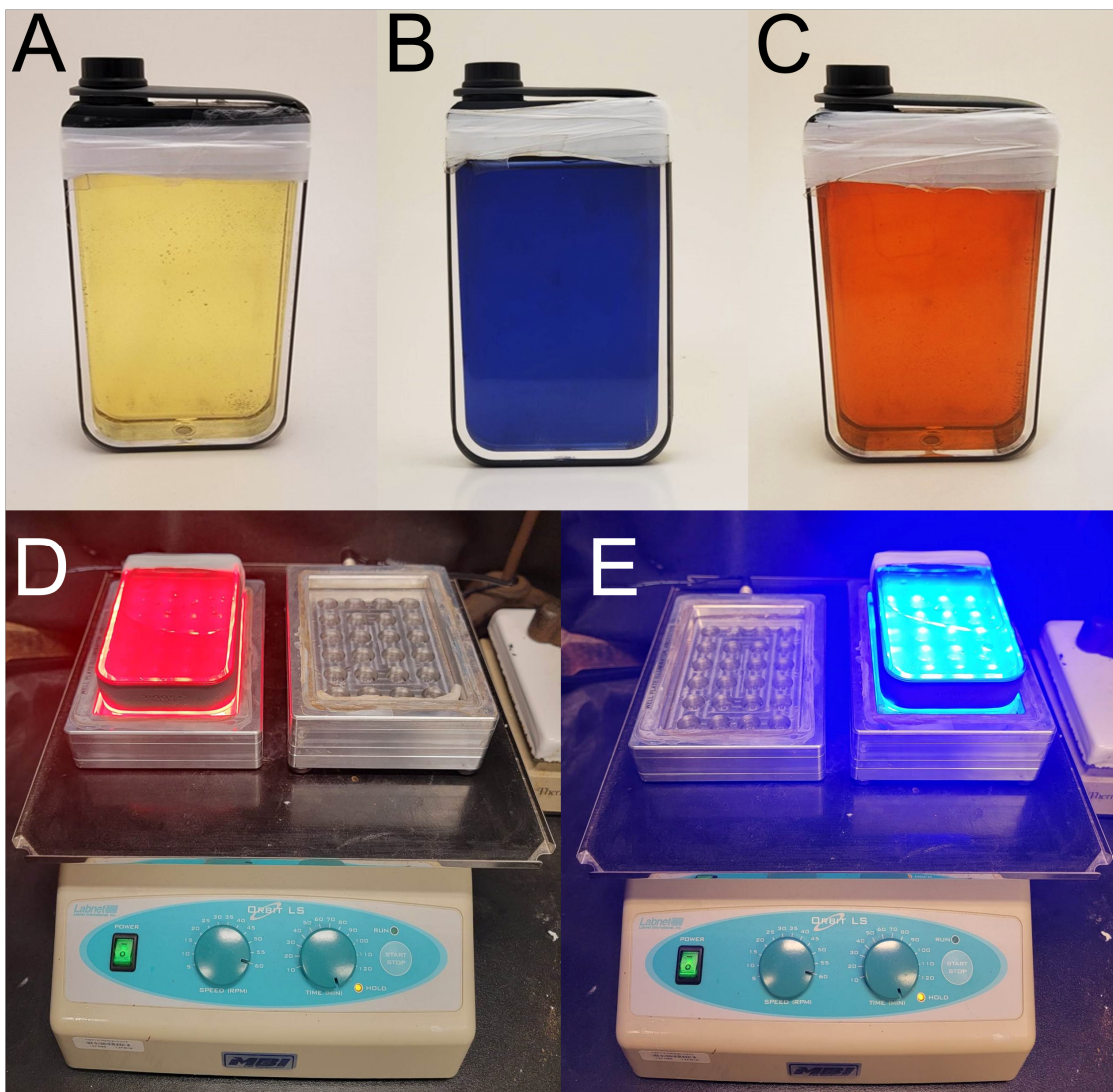


Figure S2: 200 mL batches of AgNP seeds (A), tAgNPs (B), and dAgNPs (C). D and E show the seed solutions flasks placed on the red (D) and blue (E) WPIs from Luzchem during the nanoparticle growth step. Note that illumination with the red WPI (D) leads to the sample in B, while illumination with the blue WPI (E) leads to the sample in C.

Real time absorbance acquisition -

Real time spectral acquisition was performed using two different approaches. For the dAgNPs, a 3 mL cuvette was placed in a Cary 60 equipped with a qpod 2e cuvette holder by Pacific Northwest, with an open window through which light can be directed into the AgNP seed suspension using a 450 nm LEDi by Luzchem. Measurements were taken every 20 minutes for 24 hours, with the reaction reaching completion around the 20 hour mark.

For the tAgNPs, a different approach needed to be taken due to the geometry of the light source required. A 200 mL batch of AgNPs was connected to a flow cuvette using Teflon tubing attached to a peristaltic pump to regularly flow fresh solutions from the batch into the cuvette, and then back into the batch container. Measurements were taken every 30 minutes for 48 hours, with the reaction being stopped at 48 hours.

It should be noted that due to the observation methods and lack of purification employed at each time point, there is some variability in how the collected spectra appear compared to the AgNPs used in the manuscript.

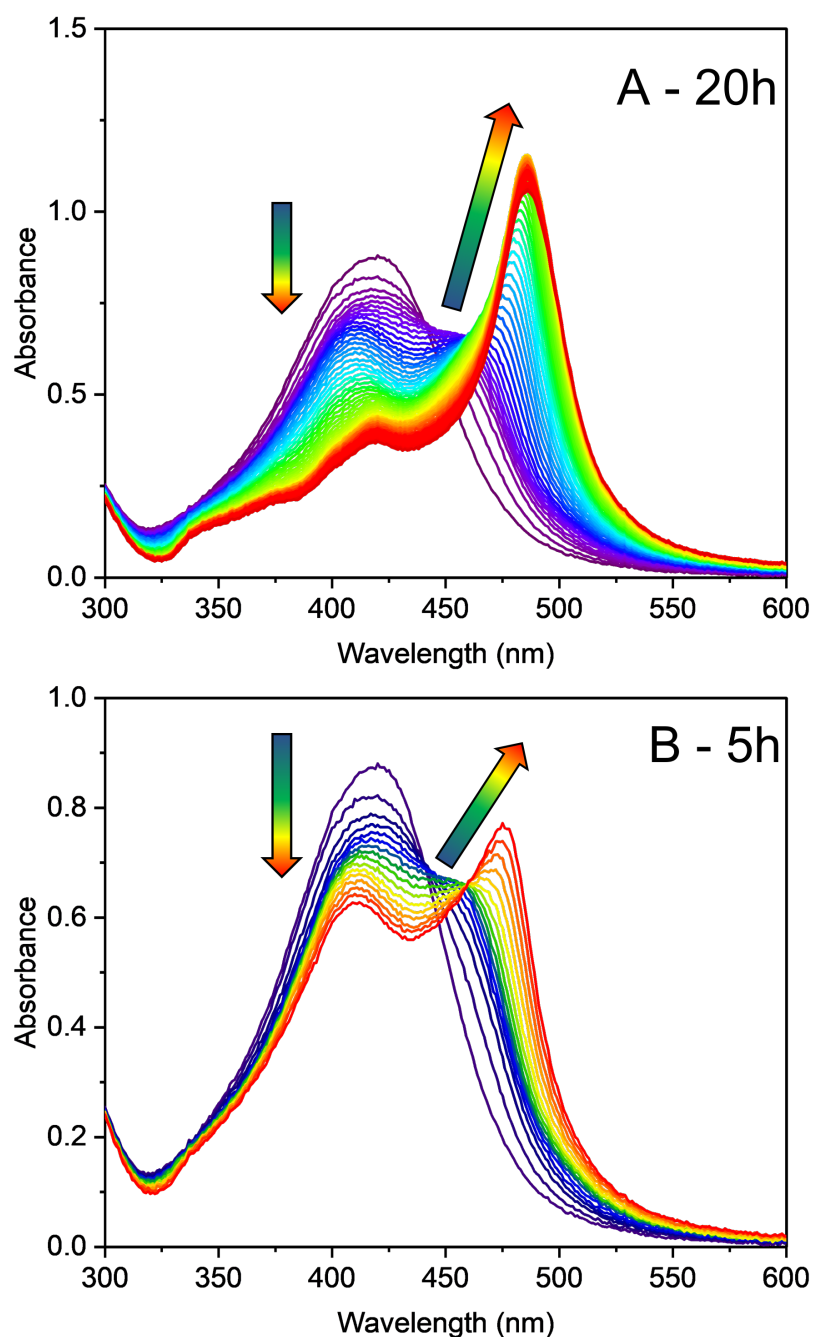


Figure S3: UV-Vis absorbance of dAgNPs, monitored in real time during AgNP growth using a modified Cary 60 UV-Vis spectrometer to simultaneously irradiate particles and measure UV-Vis absorbance of a 3 mL batch every 20 minutes. A) The total change in absorbance over 20h, arrows indicate the change in absorbance over time, from blue (t=0) to red (t=20h). B) UV-Vis absorption over the first 5h, chosen to highlight the early shifting of the AgNP wavelength away from the wavelength of the incident light source (450 nm) as the particles grow.

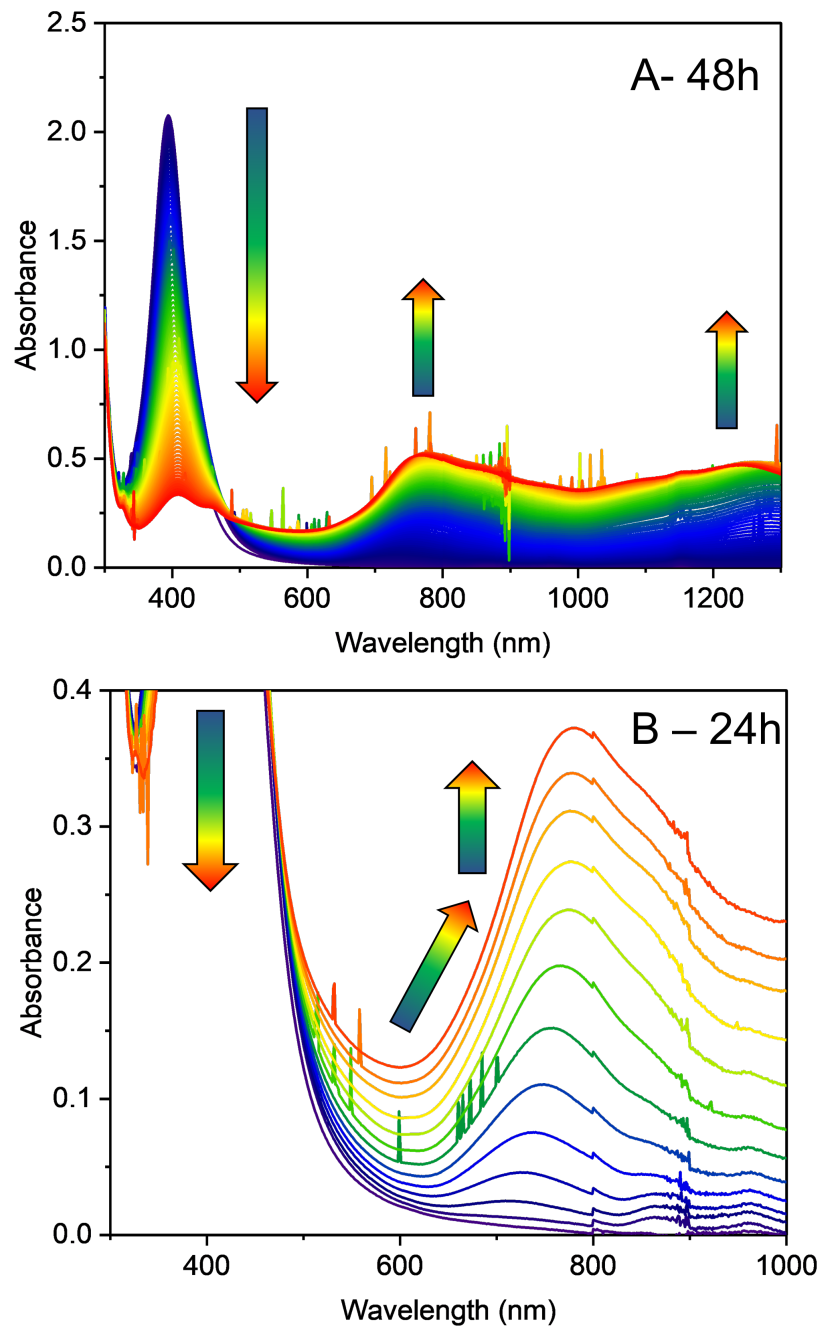


Figure S4: UV-Vis absorbance of tAgNPs, monitored in real time during AgNP growth using a closed-loop flow system adapted to a Cary 7000 UV-Vis-NIR spectrometer to simultaneously irradiate particles and measure UV-Vis absorbance of a 200 mL batch. Sharp spikes in the spectrum are caused by air bubbles in the flow system. A) The total change in absorbance over 48h, arrows indicate the change in absorbance with time, from $t=0$ (blue spectra) to $t=48h$ (red spectra). B) UV-Vis absorption over the first 24h, with traces shown for every hour.

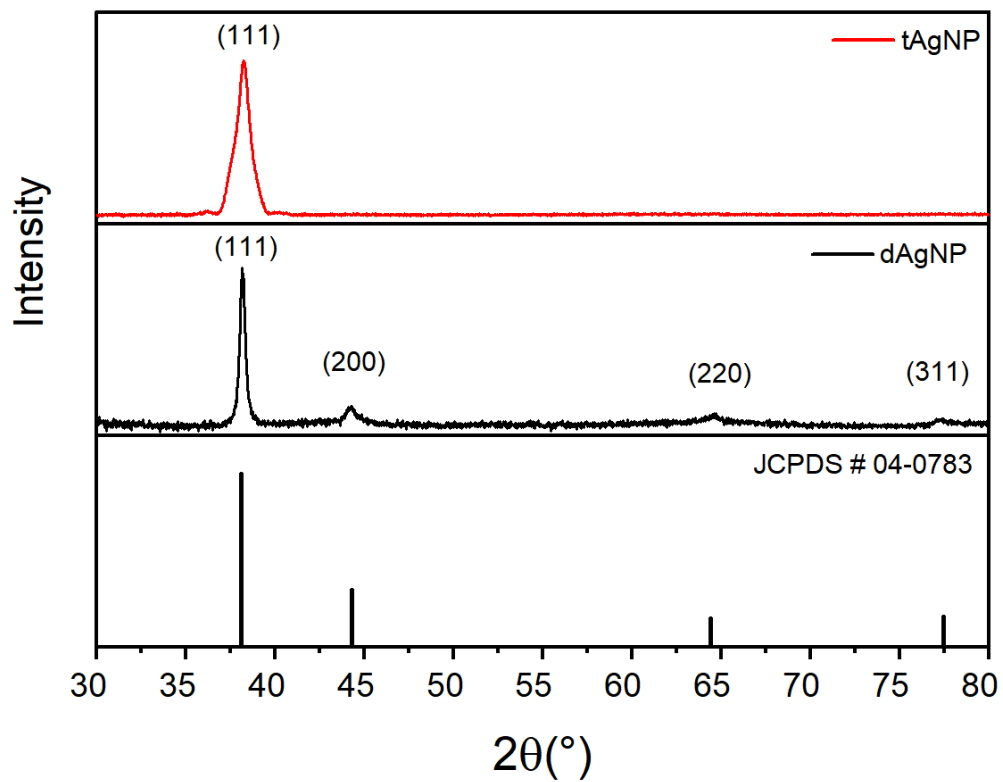


Figure S5: X-ray diffractograms of the Ag nanostructures: tAgNP (red) and dAgNP (black). In the bottom, the diffractogram pattern for metallic silver according to the JCPDS card no: 04-0783.

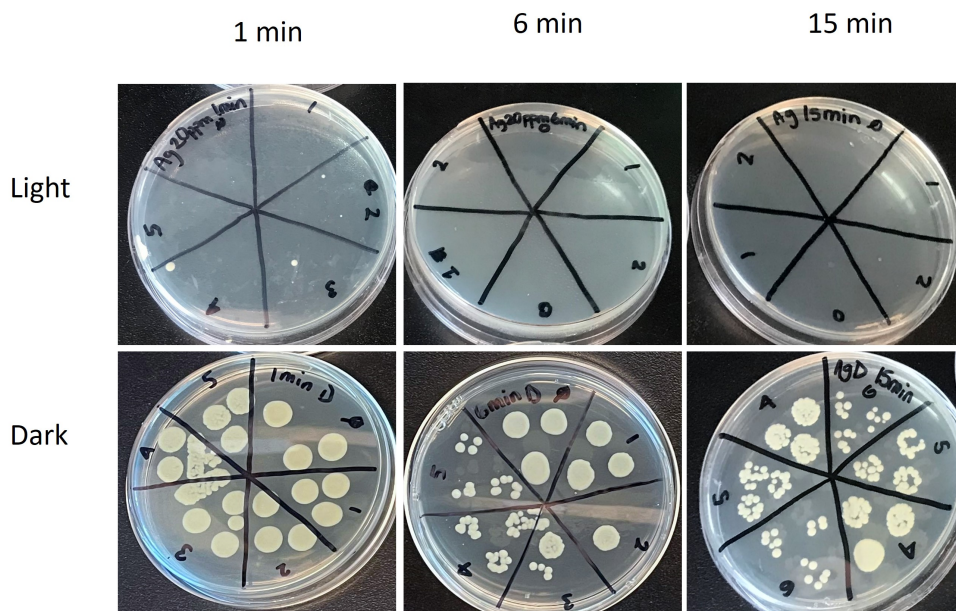


Figure S6: Antibacterial effect of tAgNPs on *E. coli*: Photographs of agar plates on which *E. coli* cells were incubated after treatment with tAgNp in the dark or under NIR irradiation (810 nm- 0.99 W/cm²) for 1 to 15 min. Each quadrant represents a 10^x dilution.

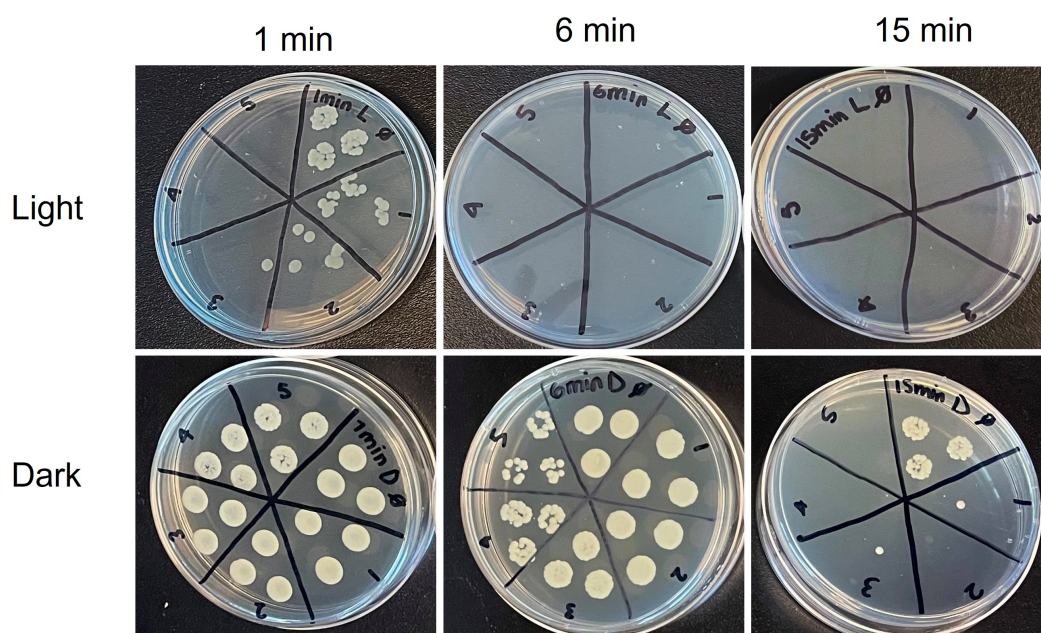


Figure S7: Antibacterial effect of dAgNPs on *E. coli*: Photographs of agar plates on which *E. coli* cells were incubated after treatment with dAgNPs in the dark or under blue irradiation (450 nm, 0.95 W/cm²) for 1 to 15 min. Each quadrant represents a 10^x dilution.

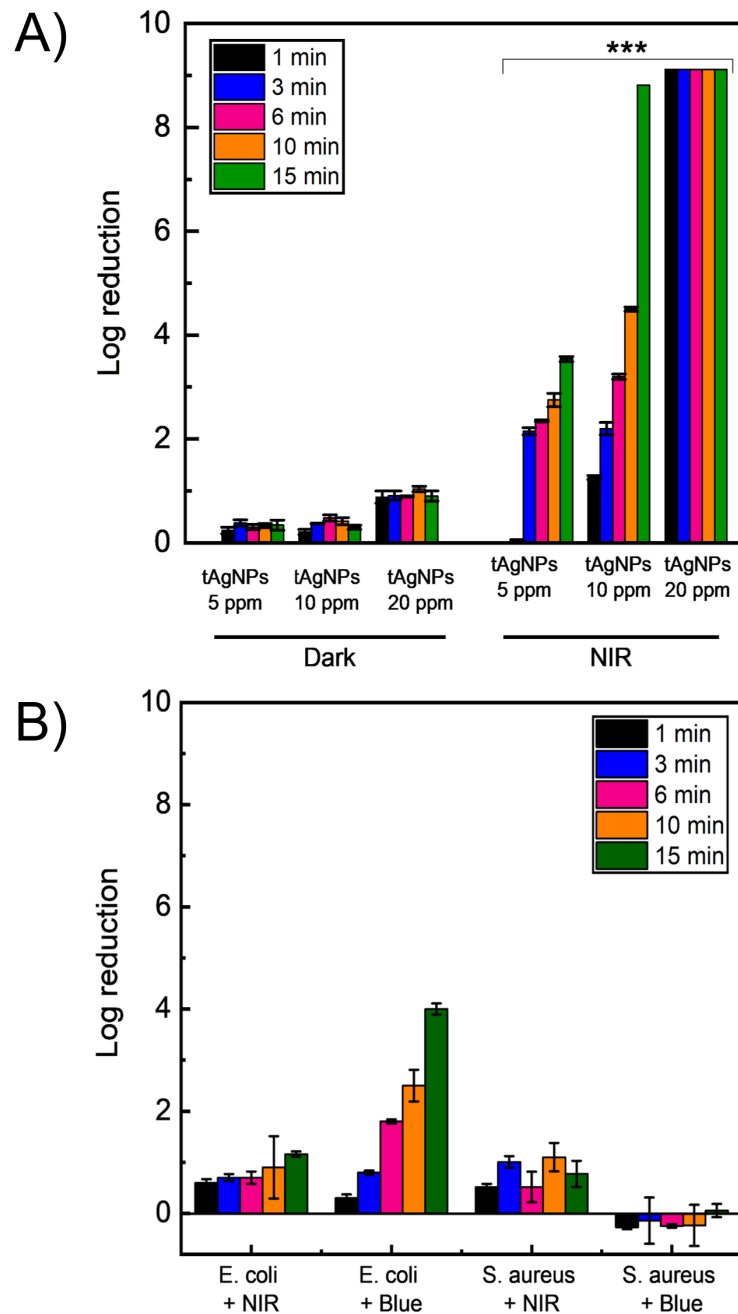


Figure S8: (a) Antibacterial activity of tAgNPs against *S. aureus* under dark and NIR irradiation. *S. aureus* cultures were treated from 1-15 min, with tAgNPs with concentrations of 5, 10 & 20 ppm. (b) Bacterial survival after irradiation with NIR LED (810 nm) or blue LED (450 nm) for up to 15 min in the absence of AgNPs. Bacterial growth was determined by the plate counting method. Error bars represent the standard deviations of the log reduction (***) $p < 0.001$.

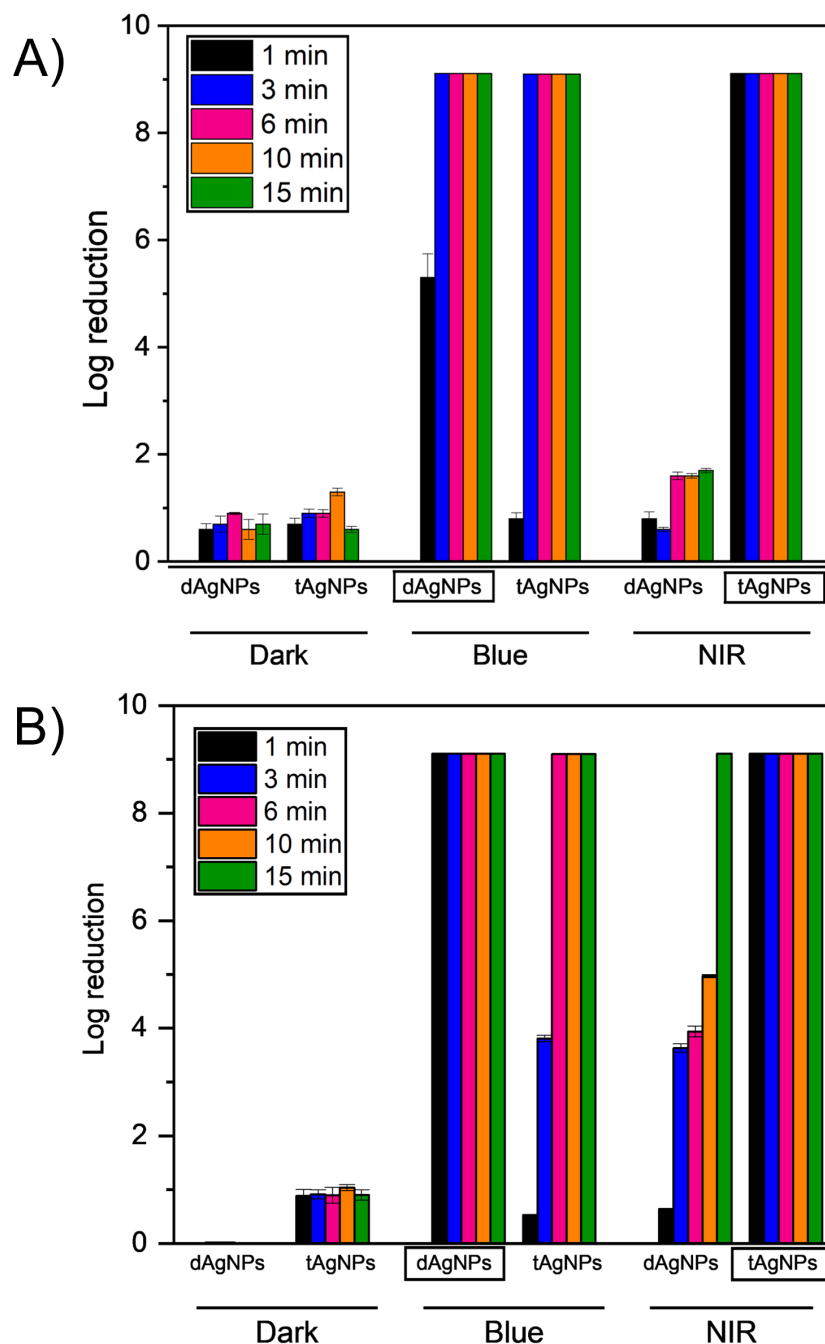


Figure S9: Antibacterial effect of tAgNPs and dAgNPs: log reduction of *E. coli* (A) and *S. aureus* (B) treated with blue light (450 nm) or with NIR (810 nm). The power density was 0.93W/cm² for blue light and 0.99 W/cm² for NIR light. Bacteria were treated with 20 ppm suspensions of the Ag nanostructures. Complementary AgNP and light are flagged with a black box. Error bars represent standard deviations of the log reduction.

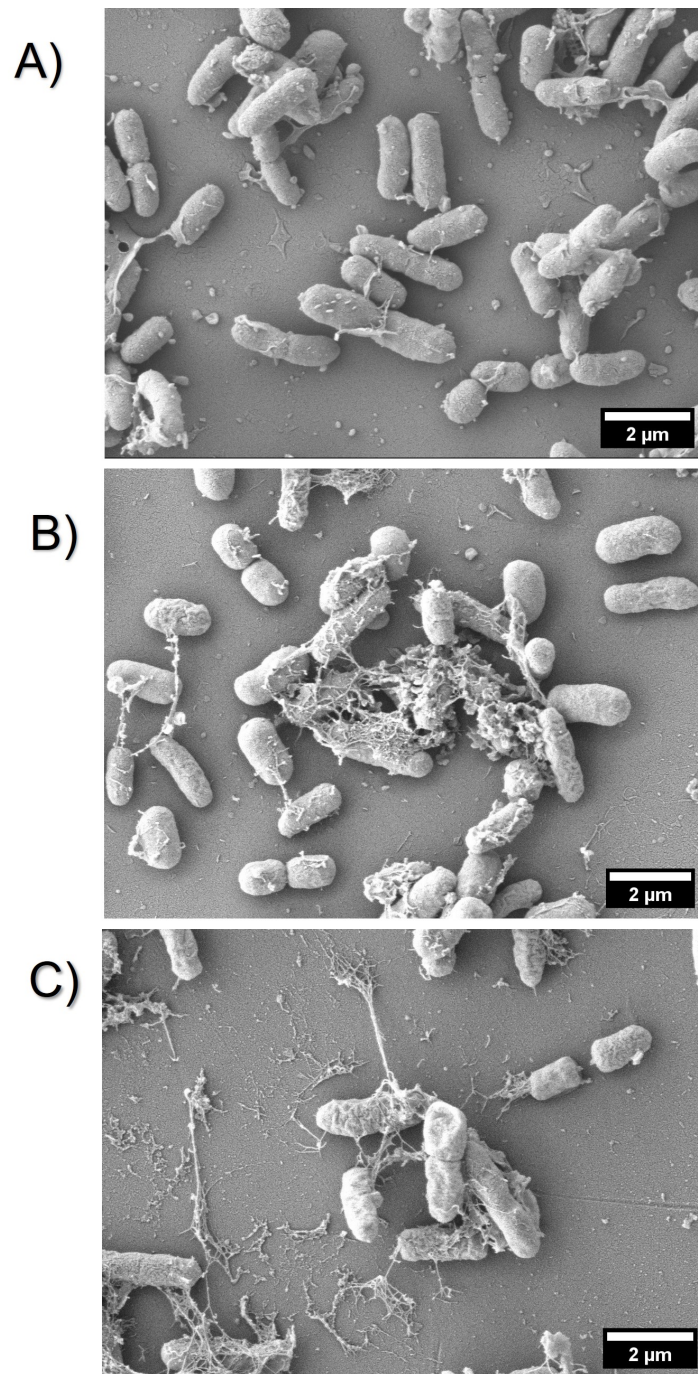


Figure S10: SEM images of *E. coli* (10^8 CFU/mL) in LB (A), treated with 20 ppm of tAgNPs and NIR irradiation (810 nm) for 1 min (B) and for 15 min (C).

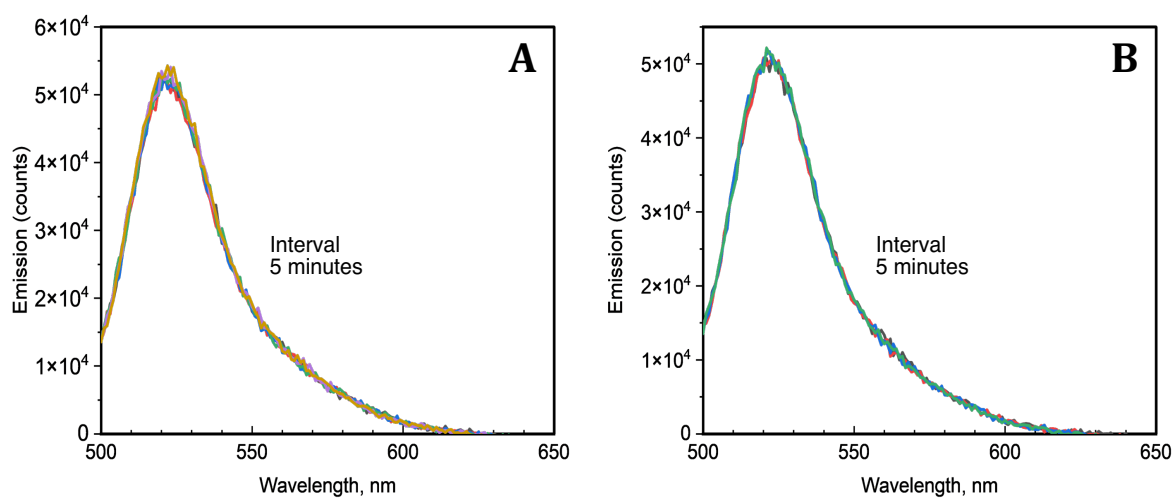


Figure S11: Emission intensity of DCF assay in the absence of AgNPs under NIR irradiation (A) and under dark conditions (B) for 15 minutes.

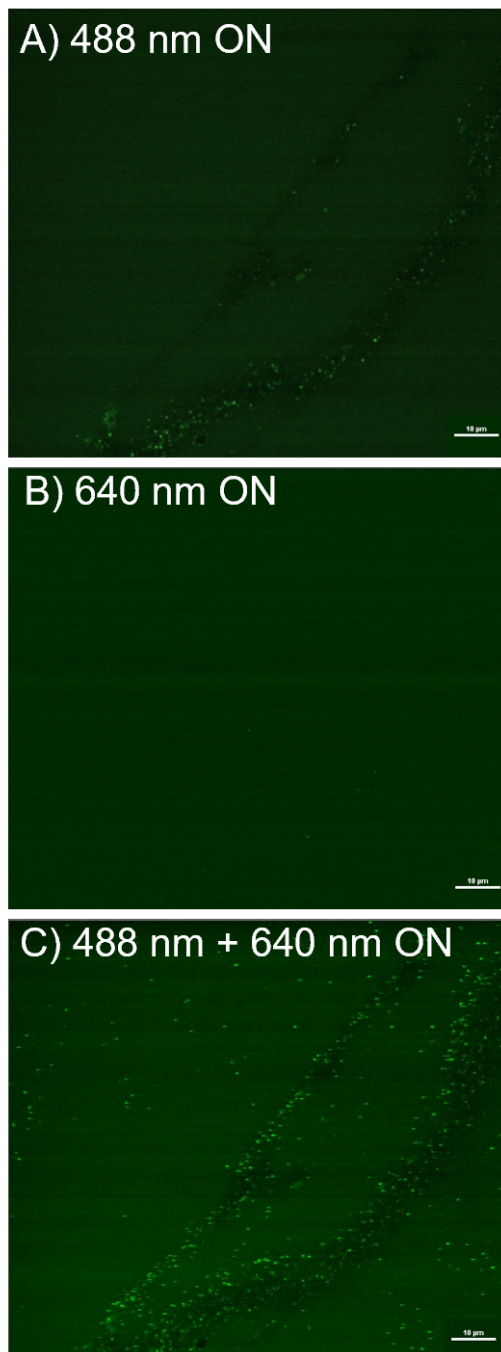


Figure S12: Confocal microscopy images of tAgNPs on a glass slide (seen as dark regions in the images) under gentle flow of fresh H₂DCF using a flow reaction system described elsewhere¹. In this system, light green bursts represent localized H₂DCF reacting with ROS/RNS to yield the emissive DCF. A) The system with only 488 nm excitation, where only background levels of DCF are expected to be seen. B) The system under 640 nm excitation, a wavelength at which the NPs can absorb, but H₂DCF does not. C) The system excited by both lasers, simultaneously exciting the tAgNPs and the dye simultaneously to yield an increase in overall emission.

Table S1: Ag ppm in supernatant of AgNP suspensions following 6h of complimentary LEDi irradiation, as determined using ICP-OES. Note that the detection limit of the instrument is 0.1 ppm.

	tAgNPs	dAgNPs
Initial Ag ppm	0.14	0.21
Ag ppm after 6h of irradiation	0.21	0.15

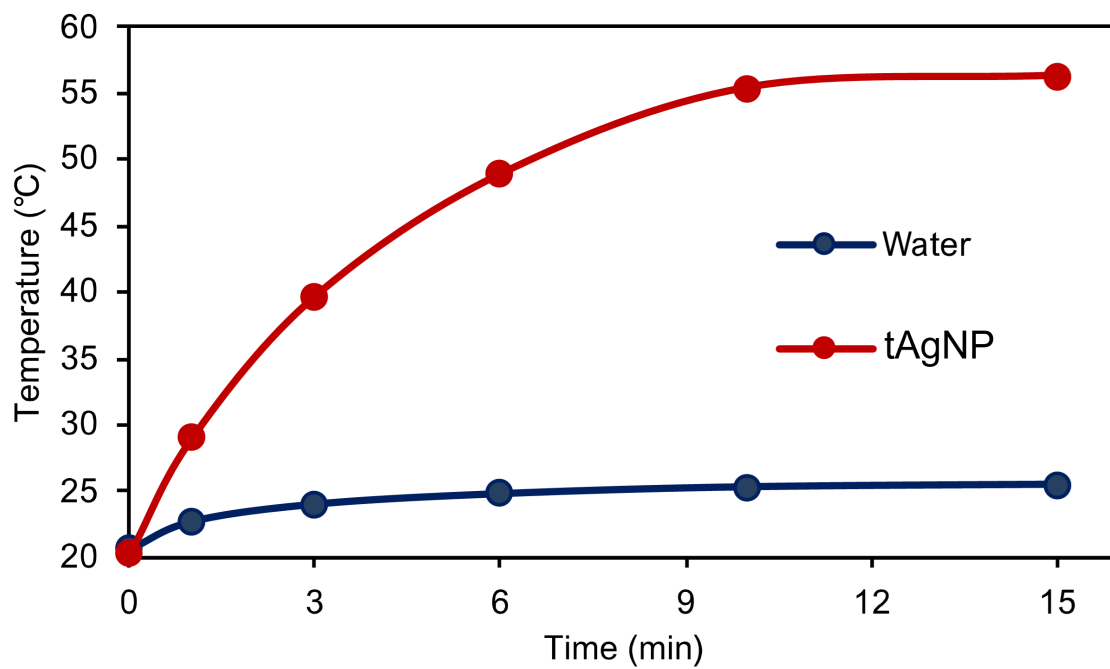


Figure S13: Temperature of water (blue) and a 10 ppm tAgNP suspension (red) over several minutes under NIR irradiation.

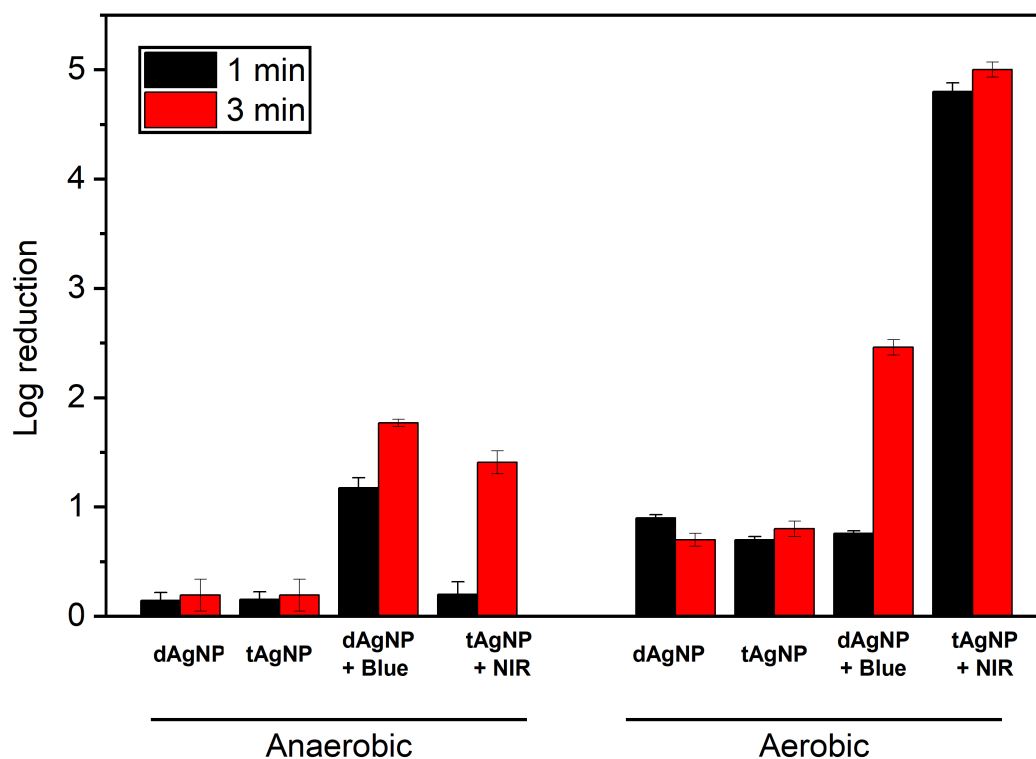


Figure S14: Effect of Oxygen on the antibacterial performance of Ag nanostructures. Log reduction of *E. coli* treated with dAgNps in the presence and absence of blue irradiation (450 nm); or with tAgNp in the presence and absence of NIR irradiation (810 nm), under air (aerobic) or N₂ atmosphere (anaerobic). The power density was 0.93W/cm² for blue light and 0.99 W/cm² and the bacteria were treated with 10 ppm of the Ag nanostructures for 1 and 3 min. Error bars represent standard deviations of the log reduction.

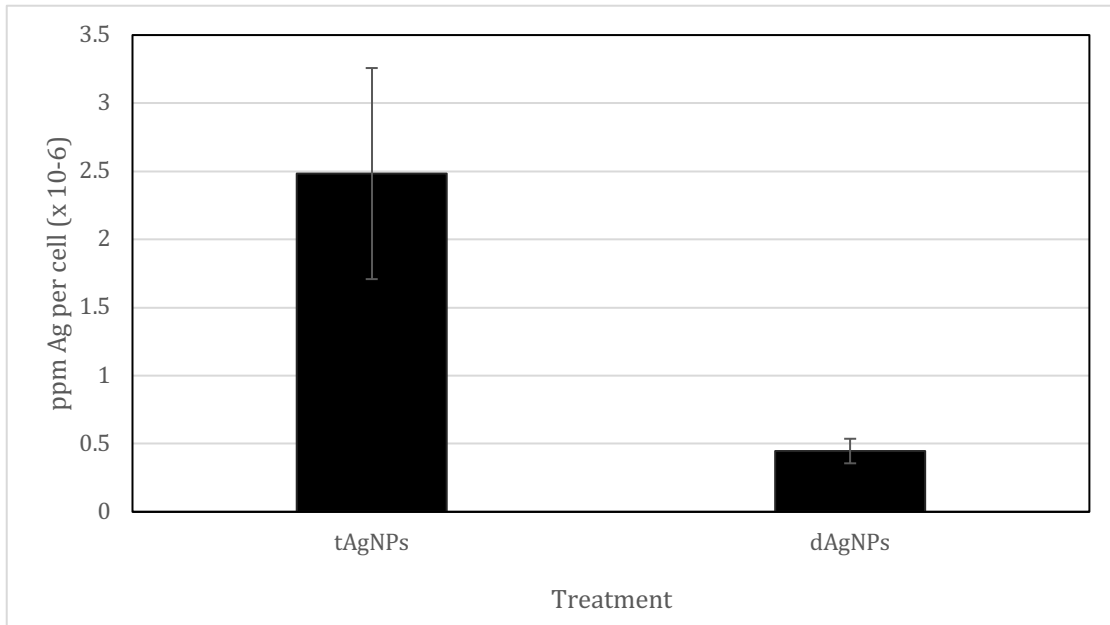


Figure S15: Ag uptake in HT-1080 cells following treatment with AgNPs, as determined by ICP-OES. Results are the average of triplicates, bars represent standard deviation.

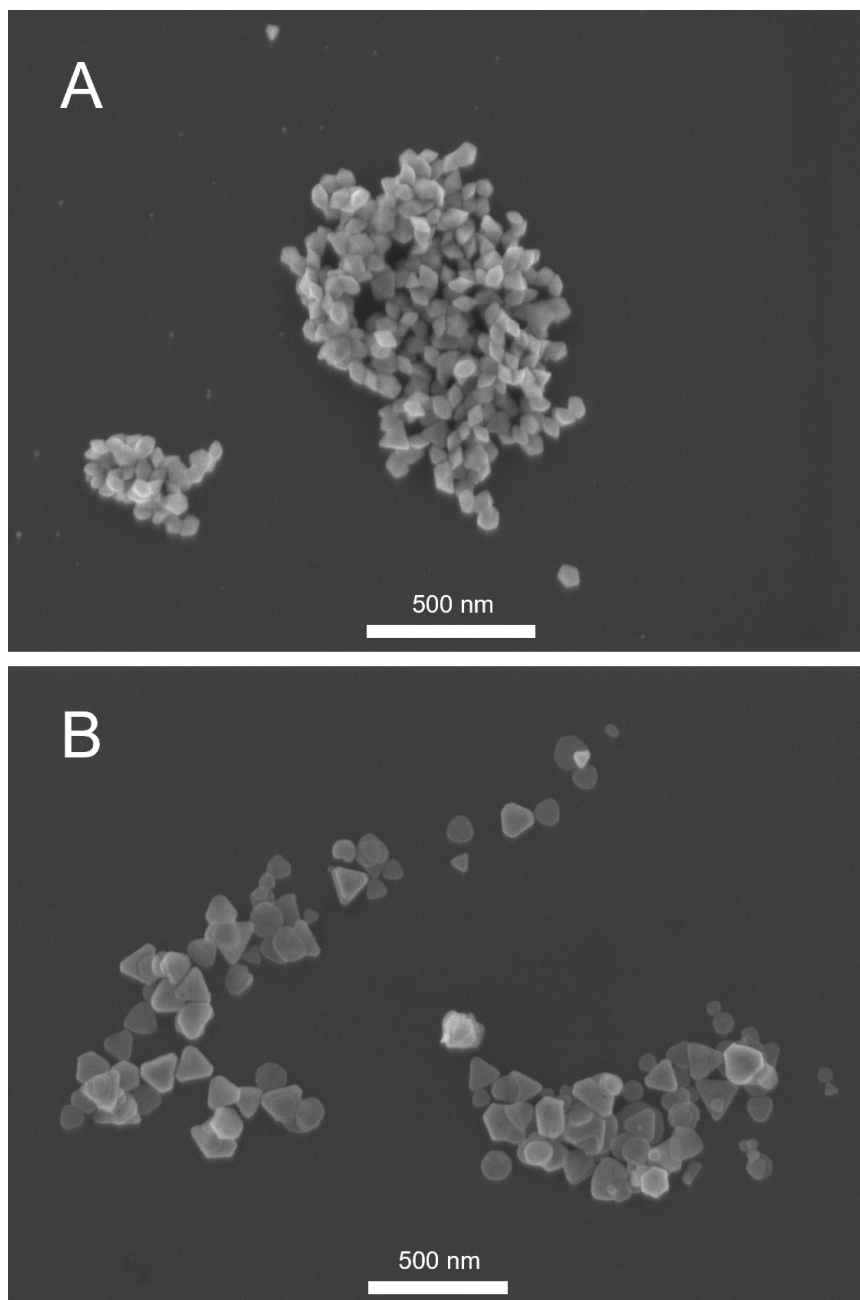


Figure S16: SEM images of (A) dAgNPs, and (B) tAgNPs. Size bars are 500 nm. Note that diamond shaped particles, as seen in A, may represent decahedral particles which are turned on their side.

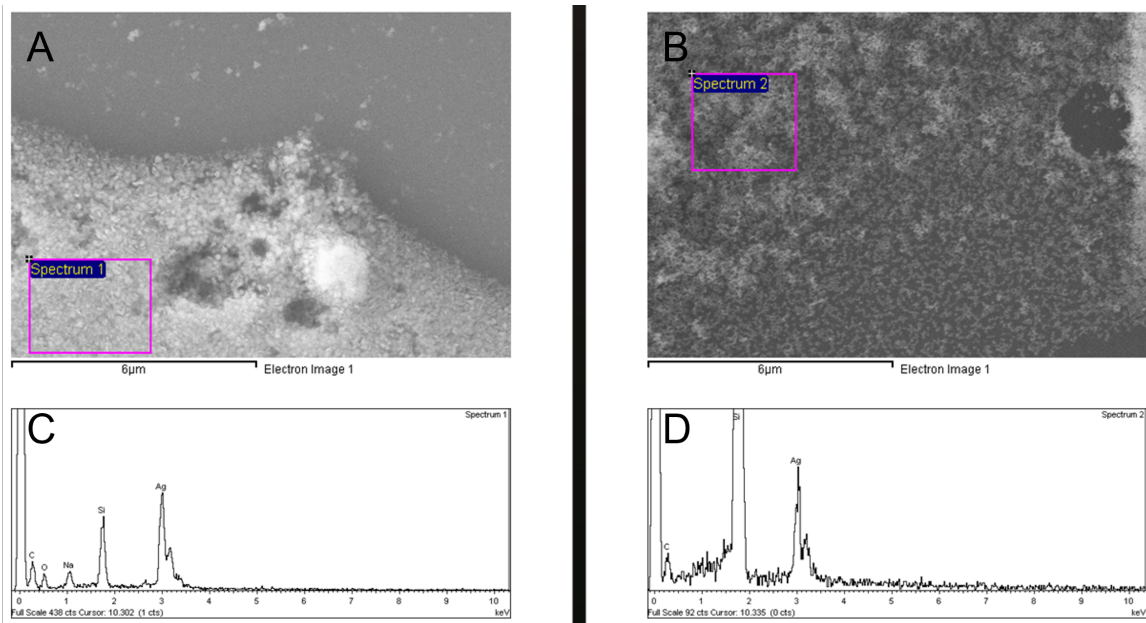


Figure S17: SEM images of densely packed regions of tAgNPs (A) and dAgNPs (B), and corresponding EDS spectra collected from these regions (C & D, respectively).

References:

- 1) B. Wang, C.R. Bourgonje, J.C. Scaiano, Fiber-glass supported catalysis: real-time, high-resolution visualization of active palladium catalytic centers during the reduction of nitro compounds. *Catal. Sci. Technol.*, 2023,13, 1021-1031